PROGRESS IN IDEAL HIGH-INTENSITY UNBUNCHED BEAMS IN ALTERNATING-GRADIENT FOCUSING SYSTEMS

Ronak Bhatt, Chiping Chen, Jing Zhou
MIT/PSFC, 77 Massachusetts Avenue, Cambridge, MA 02139, USA

Abstract

A persistent challenge in high-intensity accelerator design is the optimization of matching conditions between a beam injector and a focusing system in order to minimize non-laminar flows, envelope oscillations, emittance growth, and halo production. It has been shown [1] that the fluid motion of a thin space-charge dominated beam propagating through a linear magnetic focusing channel consisting of any combination of uniform or periodic solenoidal fields and alternating gradient quadrupole fields can be solved by a general class of corkscrewing elliptic beam equilibria. The present work extends this discussion to non-axisymmetric PPM focusing and derives conditions under which a uniform density elliptical beam can be matched to such a focusing channel by considering the fluid equilibrium in the paraxial limit. Methods of constructing such a beam are also discussed, with particular attention devoted to analytic electrode design for Pierce-type gun diodes of elliptical cross-section.

I. INTRODUCTION

The generation, acceleration and transport of a high intensity, space-charge-dominated, charged-particle (electron or ion) beam are the most challenging aspects in the design and operation of particle accelerators. In high-intensity ion and electron accelerators, beams often exhibit non-laminar flows such as large-amplitude density fluctuations [2], mismatched envelope oscillations [3], emittance growth, chaotic particle orbits, beam interception, and difficulty in beam focusing and compression. Many of these effects are due to beam mismatch or non-equilibrium behavior. Elliptic beams allow simplified and natural matching [1] between beam injectors and commonly used magnetic focusing lattices, reducing the emittance growth associated with beam mismatch. Electron beams of elongated elliptic cross-sections have also generated great interest in vacuum electronics [4] for next-generation accelerators, because of their low space-charge energy and efficient coupling to rf structures when compared to circular beams.

Despite their advantages for certain applications, elliptic beams have yet to be widely adopted, as their inherent 3D nature makes modeling elliptic diodes and transport systems particularly challenging, both analytically and numerically. In Section II we demonstrate the validity of a new analytic technique to determine the electrode shapes supporting a non-relativistic elliptic beam, which may be used independently or in conjunction with 3D modeling codes. A sample set of electrodes is computed explicitly for a 1 micro-perveance, large aspect ratio (10:1) elliptic beam diode. The geometry is tested via 3D OMNITRAK [5] simulations to show nearly ideal Child-Langmuir space-charge-limited flow with high laminarity and a constant elliptic cross-section.

The elliptic beam discussed in Sec. II can be naturally matched into a periodic quadrupole magnetic field. This is because the beam has negligibly small transverse velocity at the exit of the diode, and also because the transverse velocity of a cold-fluid beam equilibrium in a periodic magnetic quadrupole field vanishes at the time reversal symmetry point of the focusing lattice. In Section III, we discuss a novel periodic solenoidal focusing scheme which is particularly well-suited to high aspect-ratio elliptic beams.

II. ELLIPTIC DIODE DESIGN

In order to enforce Child-Langmuir [6] flow in a beam interior, the diode design problem requires solving Laplace's equation for the exterior with Cauchy boundary conditions, general solutions of which are difficult or impossible to obtain [7]. Standard solution methods fail due to the exponential growth of errors which is characteristic of all elliptic-equation Cauchy problems. Nonetheless, Pierce [8] was able to analytically solve the exterior problem for an infinite 2D sheet-beam geometry (i.e., neglecting end-effects), and Radley [9] for a beam of circular cross-section. Previous solutions of the elliptic beam problem [10], have suffered from the limitations of approximations made, obscurity, and difficulty of numerical implementation.

For the design of physical beam diodes, designers, guided by these analytic results, make use of ray-tracing codes such as the 2D EGUN [11] and 3D OMNITRAK [5], or particle-in-cell codes such as MICHELLE [12] and WARP [13]. These codes can be used as part of an iterative optimization process in order to arrive at an approximate set of external electrodes which support the desired beam cross-section. Non-axisymmetric beams present a challenge for diode designers, who must include an extra dimension in the electrode geometry optimization. We utilize here the method presented in Ref. [14] for the analytical determination of electrode surfaces.

Consider a non-relativistic charged-particle beam of length d and elliptic cross-section with semi-major axis a and semi-minor axis b, as shown in Fig. 1. The charged particles are emitted from a flat elliptic plate, held at potential $\Phi = 0$, in the $z = 0$ plane and collected by another flat elliptic plate, held at potential $\Phi = \Phi_d$, in the $z = d$ plane. The cold fluid equations describing the beam interior are

$$\partial n/\partial t + \nabla\cdot(n\mathbf{V}) = 0 \quad (1)$$

$$\partial \mathbf{V}/\partial t + (\mathbf{V}\cdot\nabla)\mathbf{V} = -(q/m)\nabla\Phi, \quad (2)$$

$$\nabla^2\Phi = -4\pi q n, \quad (3)$$

for the region $x^2/a^2 + y^2/b^2 \le 1$ and $0 \le z \le d$. In Eqs. (1)-(3), $\mathbf{V}$ is the flow velocity, and n is the density of particles, each of mass m and charge q. Note that, consistent with the non-relativistic approximation, we neglect any self-magnetic field. In the beam exterior, the potential satisfies Laplace's equation

$$\nabla^2\Phi = 0. \quad (4)$$

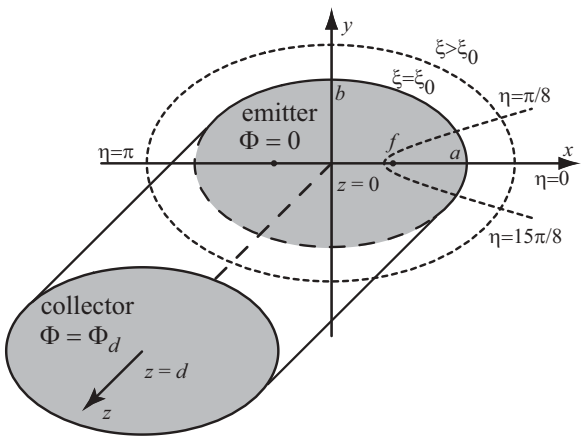

Figure 1: A beam of elliptic cross-section (semi-major axis a, semi-minor axis b) is shown in Cartesian and elliptic cylindrical coordinates. The beam is emitted from an elliptic plate at $\Phi = 0$ in the $z = 0$ plane and collected by an elliptic plate at $\Phi = \Phi_d$ in the $z = d$ plane. The beam fills the area enclosed by the surface $\xi = \xi_0$. In any z-plane, lines of constant ξ are ellipses, and lines of constant η are semi-hyperbolas.

The steady-state solution to the interior problem defined by Eqs. (1)-(3) can be obtained by using the plate potentials as boundary conditions for Poisson's equation and imposing the constraint that particles emerge from the $\Phi = 0$ emitter with zero velocity, i.e. the space-charge-limited boundary condition. This results in the well-known 1D Child-Langmuir (C-L) [6] solution for laminar, space-charge-limited flow with $\Phi(z) = \Phi_d(z/d)^{4/3}$ and $n\mathbf{V} = \hat{\mathbf{e}}_z\left(2q{\Phi_d}^3/m\right)^{1/2}/\left(9\pi d^2\right)$. For example, an electron diode of length $d = 5.2$ mm and diode voltage $\Phi_d = 5$ kV produces a current density of $3\ \mathrm{A/cm^2}$.

To determine the potential distribution in the beam exterior, we solve Laplace's equation (4) while matching the interior and exterior electric fields on the elliptic beam boundary. From the C-L solution, the matching conditions on the elliptic beam boundary imply, for $0 \le z \le d$,

$$\Phi\big|_{\text{beam boundary}} = \Phi_d(z/d)^{4/3}, \quad (5)$$

$$(\hat{\mathbf{n}}\cdot\nabla)\Phi\big|_{\text{beam boundary}} = 0, \quad (6)$$

where $\hat{\mathbf{n}}$ is a unit vector normal to the elliptic beam boundary $x^2/a^2 + y^2/b^2 = 1$. We aim to find exterior equipotential surfaces corresponding to the emitter and collector potentials $\Phi = 0$ and $\Phi = \Phi_d$, respectively. If electrodes at the given potentials are made to lie along these surfaces, they will enforce the conditions in Eqs. (5) and (6) on the interval $0 \le z \le d$.

It is useful to introduce the elliptic cylindrical coordinate system (ξ, η, z), i.e. $x = f\cosh(\xi)\cos(\eta)$, $y = f\sinh(\xi)\sin(\eta)$, where $0 \le \xi < \infty$ is a radial coordinate, $0 \le \eta < 2\pi$ is an angular coordinate, and $f = \sqrt{a^2 - b^2}$ is the distance from the center of the ellipse to either of its foci, as illustrated in Fig. 1. The elliptic beam boundary is specified by the surface $\xi = \xi_0 = \coth^{-1}(a/b)$. Separating variables in these coordinates, Eqs. (4)-(6) can be solved as in Ref. [14] to yield the exterior potential

$$\Phi(\xi,\eta,z) = \int_C dk A(k) e^{kz} G(kf,\xi,\eta), \quad (7)$$

where

$$A(k) = \frac{\Phi_d d^{-4/3}}{\Gamma\left(-\frac{4}{3}\right)}\frac{i}{2\sin\left(\frac{4\pi}{3}\right)}k^{-7/3}, \quad (8)$$

$G(kf,\xi,\eta)$ is the boundary-conforming Mathieu function solution defined in Ref. [14], and a Hankel contour [15] is used for the integration.

In order to verify the theory, we use a numerical root-finding technique to determine the $\Phi = 0$ and $\Phi = \Phi_d$ equipotentials of Eq. (7) for a particular example – a 10:1 elliptical beam with $\Phi_d = 5.0$ kV, $d = 5.2$ mm, $a = 6.0$ mm, and $b = 0.6$ mm. The equipotential surfaces are input as boundary conditions for a 3D space-charge emission simulation using OMNITRAK [5], a commercial available ray-tracing code. The simulation predicts the effective beam temperatures $T_{eff,x} = 6.7\times10^{-4}$ eV and $T_{eff,y} = 8.1\times10^{-3}$ eV. These temperatures are negligible compared to a typical thermionic diode temperature of ~0.1 eV, implying that the emittance of an elliptical diode constructed using the above prescription will approach the theoretical limits imposed by finite emitter temperature.

III. PERIODIC SOLENOIDAL FOCUSING

For a high-brightness, space-charge-dominated beam, kinetic (emittance) effects are negligibly small, and the beam can be adequately described by the cold-fluid equations

$$n\left(c\beta\frac{\partial}{\partial s} + \mathbf{V}_\perp\cdot\frac{\partial}{\partial \mathbf{x}_\perp}\right)\mathbf{V}_\perp = \frac{qn}{\gamma m}\left[-\frac{1}{\gamma^2}\nabla_\perp\Phi + \beta\hat{\mathbf{e}}_z\times\mathbf{B}_\perp^{\text{ext}} + \frac{\mathbf{V}_\perp}{c}\times B_z^{\text{ext}}(s)\hat{\mathbf{e}}_z\right], \quad (9)$$

$$c\beta\frac{\partial n}{\partial s} + \nabla_\perp\cdot(n\mathbf{V}_\perp) = 0, \quad (10)$$

$$\nabla_\perp^2 \Phi = \beta^{-1} \nabla_\perp^2 A_z = -4\pi q n, \qquad (11)$$

where $s = z$, $\gamma = \left(1-\beta^2\right)^{-1/2}$ is the relativistic mass factor, use has been made of $\beta_z \cong \beta = \text{const}$, and the electric and magnetic fields are given by $\mathbf{E} = -\nabla\Phi$ and $\mathbf{B} = \mathbf{B}^{\text{ext}} + \nabla \times A_z \hat{\mathbf{e}}_z$. We seek solutions of the form

$$n(\mathbf{x}_\perp, z) = \frac{\lambda}{\pi a(s) b(s)} \begin{cases} 1, & 0 < 1 - \dfrac{\tilde{x}^2}{a^2(s)} - \dfrac{\tilde{y}^2}{b^2(s)}, \\ 0, & \text{otherwise} \end{cases} \qquad (12)$$

where λ is the line charge density and $(\tilde{x}, \tilde{y})$ is the transverse displacement in a rotating frame defined by $\tilde{x} = x\cos\theta(s) + y\sin\theta(s)$ and $\tilde{y} = y\cos\theta(s) - x\sin\theta(s)$.

Taking a paraxial, non-axisymmetric periodic solenoidal magnetic field, one can derive a set of envelope equations for the beam major and minor radii and internal velocities. The envelope equations are derived and solved in Ref. [16] for the transport of a uniform density elliptic beam. The nearly constant envelope solutions are plotted in Fig. 2 for a matched 6mm × 0.6mm elliptic beam.

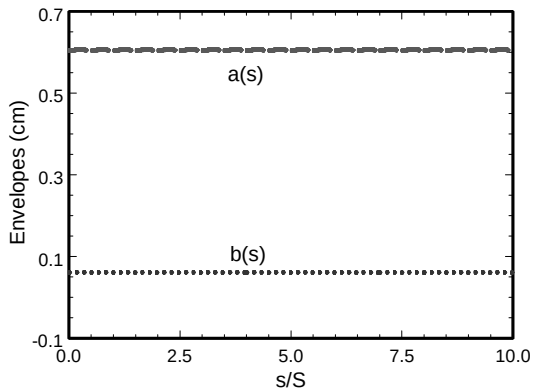

Figure 2: Beam envelopes $a(s)$ and $b(s)$ plotted over 10 lattice periods S of a non-axisymmetric periodic solenoidal magnetic field.

Compared to a magnetic quadrupole focusing scheme, the transverse excursions of beam particles are clearly much smaller in the non-axisymmetric periodic solenoidal magnetic lattice, which may imply reduced beam temperature and halo growth. The transverse velocities (not plotted), vanish at $s = 0$, which allows precise matching to the parallel-flow Child-Langmuir beam from the diode. The angular wobble $\theta(s)$ for the matched beam amounts to only a few degrees, and the addition of higher longitudinal harmonics to the focusing field may reduce the wobble magnitude further. Future work will involve PIC simulations of transport in this channel to study these issues further.

IV. CONCLUSIONS

An elliptic beam system possesses a number of potential advantages for high-intensity beam applications. We showed that high-intensity laminar flow elliptic diodes can be designed analytically, and the beams are naturally matchable into a periodic quadrupole magnetic focusing field or a non-axisymmetric periodic solenoidal focusing field. The axial variation of the equilibrium flow in the non-axisymmetric periodic solenoidal field is far less than that induced by quadrupole focusing, which suggests the beam may be more resistant to emittance and halo growth during transport. The reduced self-electric field of an elliptic beam compared to a round or average round one eases the field requirements for transverse focusing and also permits greater longitudinal compression.

The results presented here on diode design and equilibrium flow are promising, but further theoretical and simulation work is needed to clarify some of these issues regarding beam matching, halo growth, and fringe field effects.

ACKNOWLEDGEMENTS

This work was performed under the auspices of the U.S. Department of Energy, the Air Force Office of Scientific Research, and the MIT Deshpande Center for Innovation.

REFERENCES

[1] C. Chen. R. Pakter, and R.C. Davidson, Nucl. Inst. And Methods **A 464**, 518 (2001).
[2] S. Bernal, *et al.*, Phys. Plasmas **11**, 2907 (2004).
[3] T.P. Wangler, *et al.*, Nucl. Inst. & Methods **A 519**, 425 (2004).
[4] M.A. Basten and J.H. Booske, J. Appl. Phys. **85**, 6313 (1999).
[5] OMNITRAK software, copyright Field Precision, Albuquerque, NM.
[6] C.D. Child, Phys. Rev. **32**, 492 (1911); I. Langmuir, *ibid*. **21**, 419 (1923).
[7] P. Morse and H. Feshbach, *Methods of Theoretical Physics* (McGraw Hill, 1953), Vol. **1**, Chap. 6, p.702.
[8] J.R. Pierce, *Theory and Design of Electron Beams, 2nd ed.* (D. Van Nostrand Company, 1954).
[9] D.E. Radley, J. Electron. Control **4**, 125 (1957).
[10] A. Nakai, Nucl. Inst. & Methods **54**, 57 (1967).
[11] W.B. Hermannsfeldt, "Electron Trajectory Program," SLAC **226** (1979).
[12] J. Petillo *et al.*, IEEE Trans. Plasma Science **30** (3), 1238 (2002).
[13] D. P. Grote, A. Friedman, I. Haber, W. Fawley, J.L. Vay, Nucl. Inst. & Methods **A 415**, 428 (1998).
[14] R. Bhatt and C. Chen, Phys. Rev. Lett., submitted July 2004.
[15] See Ref. 7, Vol. **1**, Chap. 4, p.421.
[16] J. Zhou and C. Chen, manuscript in preparation (2004).